99. The Influence of Molecular Host Lattices on Electronic Properties of Orbitally (Near-) Degenerate Transition Metal Complexes

by **John H. Ammeter, Linus Zoller, Jürg Bachmann, Philippe Baltzer, Eduard Gamp, René Bucher** and **Erich Deiss**

Institute of Inorganic Chemistry, University of Zürich, Winterthurerstrasse 190, CH-8057 Zürich

Herrn Prof. Dr. *Conrad Hans Eugster* zum 60. Geburtstag gewidmet

(13.III.81)

Summary

Transition metal complexes often have low-lying excited electronic states and, as a consequence, tend to be *electronically labile, i.e.*, their electronic properties exhibit pronounced sensitivity to external perturbations. Often drastic changes in various spectroscopic properties indicating substantial electronic rearrangements can be induced by relatively weak intermolecular forces as provided by nonpolar solvents or solid molecular host lattices. This behaviour can be explained by crossing of potential surfaces in the vicinity of the absolute minimum. Many physical properties of a given orbitally (near-) degenerate system depend strongly on the relative magnitude of some characteristic parameters determining the shape of the ground *Born-Oppenheimer* potential surface(s), *e.g.* barrier height *versus* zero-point energy, distance between minima *versus* zero-point amplitude, energy difference between minima, *etc.* Typical examples are systems exhibiting *Jahn-Teller* activity, spin-crossover, mixed valence, exchange coupling and other types of electronic near-degeneracies. In paramagnetic systems changes in the electronic wavefunction can be most conveniently detected and analyzed by using EPR. spectroscopy.

In paramagnetic sandwich complexes we studied two types of orbital degeneracies: *Jahn-Teller* degeneracies (d^7-systems such as $Co(cp)_2$, $Ni(cp)_2^+$ and Fe(cp) (bz), low-spin d^5-systems such as $Mn(cp)_2$) and *low-spin/high-spin equilibria* (d^5-systems such as $Mn(cp)_2$). By diluting these complexes and ring-substituted derivatives in a large variety of diamagnetic host systems we have been able to control the $^6A/^2E$ equilibrium of $Mn(cp)_2$ by influencing the metal-to-ring distance and by changing the degree of ring alkylation; similarly we have been able to vary the relative weights of the two electronic states contributing to the two-fold degenerate electronic ground state of d^5- and d^7-systems to a large degree by variation of the local asymmetric fields offered by the lattice sites of the host systems.

For comparison the electronic ground state properties of octahedral Cu (II) complexes with CuN_6 and CuO_6 chromophores, of $V(CO)_6$ and tetrahedral VCl_4 were

0018-019X/81/4/1063-20$01.00/0

also studied by EPR. between 4K and room temperature in several host systems. Characteristic differences in the details of the temperature and host dependence of the EPR. spectra in all these electronically labile systems can be explained in terms of differences in the vibronic coupling type ($E \otimes e$ *vs.* $T \otimes e,t$), the strength of linear and/or quadratic *JT*-coupling and the effects produced by spin-orbit coupling.

1. Introduction. – *1.1. Orbital (Near-) Degeneracy and Electronic Lability.* Molecular systems with unbalanced occupation of energetically close lying orbitals show pronounced sensitivity of all electronic properties towards external perturbations, caused by (real or avoided) crossings of potential surfaces in the vicinity of the absolute minimum [1], as shown schematically in *Figure 1*, case C. In condensed phases one observes a characteristic dependence of electronic observables on the nature of the solid or liquid solvent, on pressure and on temperature. Abundant examples for electronic lability are found in transition metal complexes exhibiting *Jahn-Teller* activity [2–6], spin crossovers [7–9], mixed

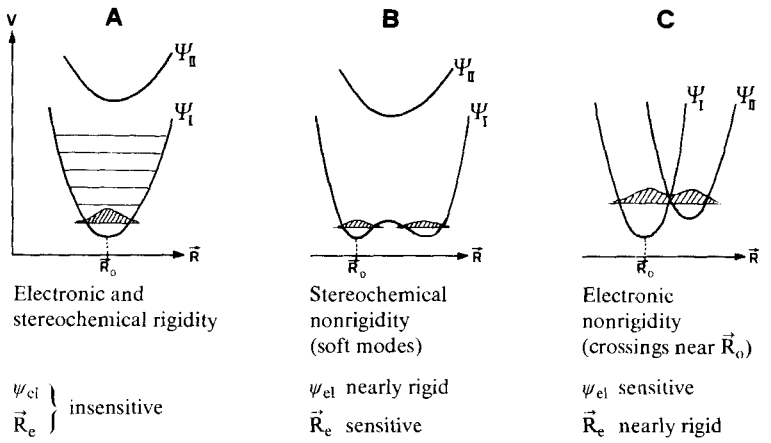

Fig. 1. *Electronic and stereochemical (non-) rigid behaviour towards changes of temperature and external perturbations* (*e.g.* solvent effects). One-dimensional cross section through potential surfaces $V(\vec{R})$ of free molecules along the most *active* internal coordinates.

Table 1. *Examples for electronic lability*

Classification	Origin of crossings	Symmetry of $\vec{R}$	Typical examples
Jahn-Teller Effect	Symmetry	Mostly degenerate	Many cubic ML_4 or ML_6 complexes
Spin crossover	$\Delta E_{LF} \approx \Delta V_{ee}$	Totally symmetric	$Fe(II)L_6/Fe(III)L_6$
Exchange coupling	Weakness of coupling between localized subsystems	Totally symmetric	$Cu(II)\langle^{L}_{L}\rangle Cu(II)$
Mixed Valence		Anti-symmetric	Ru(II)-L-Ru(III)
Others	'Accidental'	Totally symmetric	$Co(II)O_2N_2+L$

valence [10–13], exchange couplings [14–17] and other types of accidental electronic degeneracies [18] *(Table 1)*.

In the four latter cases the active coordinate $\vec{R}$ is usually nondegenerate, *i.e.* for a discussion of the electronic properties a one-dimensional cross section through the (3N-6)-dimensional potential-energy surface $V(\vec{R})$, as shown in *Figure 2*, is usually

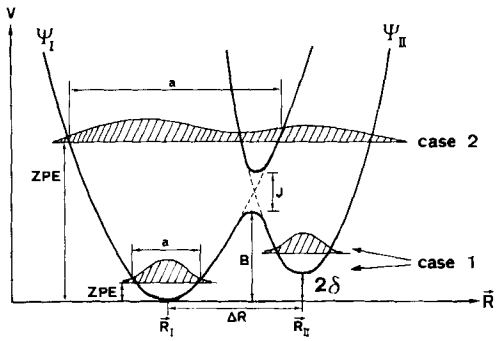

Case 1 (ZPE < B, a < ΔR)

Localized at low T
Delocalized at high T

$\psi = \Phi_{I}\chi_{I}$ or $\Phi_{II}\chi_{II}$

(*Born-Oppenheimer* product)
Discontinuous change with δ

Case 2 (ZPE > B, a > ΔR)

Delocalized at any T

$\psi = c_I\Phi_{I}\chi_{I} + c_{II}\Phi_{II}\chi_{II}$

(Vibronic superposition)
Continuous change with δ

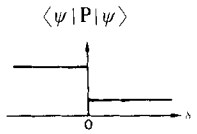

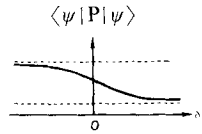

Fig. 2. *Localized and delocalized behaviour.* Influence of zero-point energy on the nature of the lowest vibronic state and on the δ-dependence of the electronic observables P. Schematic one-dimensional cross section through $V(\vec{R})$ of an electronically labile system along the most active mode (ZPE = zero-point energy, a = vibrational amplitude, $a^2/2 = \langle\chi|R^2|\chi\rangle - \langle\chi|R|\chi\rangle^2$).

sufficient. In the *Jahn-Teller* case the *active* coordinate $\vec{R}$ is normally at least two-fold degenerate, *i.e.* one has to deal with potential surfaces of the kind shown in *Figure 3*.

Figure 2 shows that the nature of the vibronic ground state of an electronically labile system depends *both* on the relevant *potential* parameters (force constants for the two minima, barrier hight B, electronic coupling *J*, nuclear displacement ΔR and energetic asymmetry 2δ) and on the effective mass associated with the active mode R, *i.e.* on the zero-point energy (relative to B) and on the zero-point amplitude a (relative to ΔR). In the case of small zero-point effects (ZPE $\ll$ B, a $\ll \Delta$R) localized behaviour, in the case of large zero-point effects (ZPE $\gtrsim$ B, a $\gtrsim \Delta$R) delocalized behaviour is expected [1]. In the case of two or more dimensions the situation is somewhat different *(Fig. 3)*: since the minimum-energy pathway between equivalent minima no longer leads through the crossing point E_0 now the size of the angular

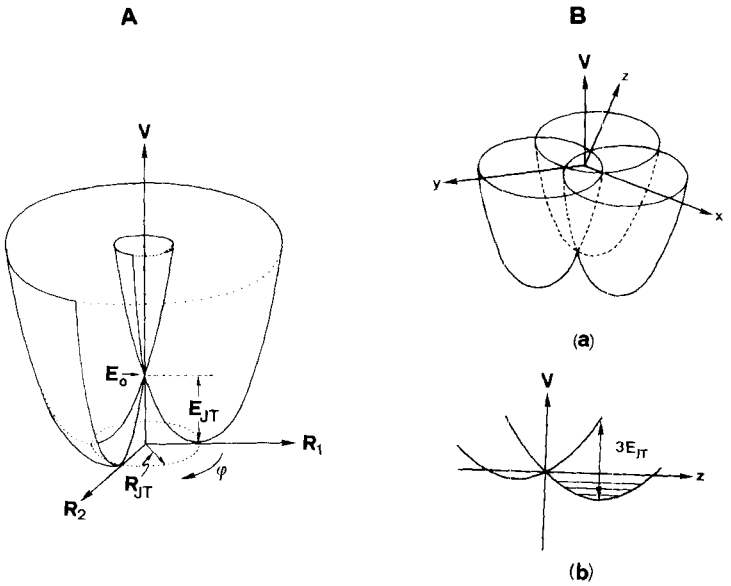

Fig. 3. A. *Two-dimensional cross section through the potential-energy surface for the case of linear* Jahn-Teller *coupling of a doubly degenerate electronic state with one single active doubly degenerate vibration.* The difference between E_o and the energy along the circular valley is the *Jahn-Teller* stabilization energy E_{JT}.

B. a) *Potential surface for an orbital triplet interacting with an e vibrational mode* (after [2]). The three minima correspond to static distortions along three equivalent axes.

b) *Section through* Figure (a) *along the z-axis.*

barriers relative to the ZPE decides about the rigidity or fluxionality of the circular coordinate [2].

In this paper we demonstrate that by systematic studies of the solvent-dependence of electronic observables (*e.g.* EPR. parameters, magnetic susceptibility, optical spectra) of labile systems at sufficiently low temperatures one can characterize the nature of the vibronic ground state and estimate the size of the relevant potential parameters.

1.2. Solvent effects in liquid and solid solutions. In the case of weakly interacting nonpolar solvents the solvent effects can be described by an additive lattice potential V_L [1] [19], see *Figure 4.* In the case of liquid solution, V_L is time-dependent, *i.e.* the solvents will have a broadening or an averaging effect on observable quantities, depending on the time scale of the experiment. Therefore it is more advantageous to study solid solutions. In the case of (near-) degeneracy the asymmetry parameter δ of the free molecule is zero (very small). The addition of a smooth solvent potential $V_L(\vec{R})$ will therefore have the strongest (relative!) influence on δ unless V_L happens to be symmetric with respect to the active coordinate R with origin at the (avoided) crossing point [19]. This gives us a handle for the experimental investigation of the nature of the vibronic state of orbitally degenerate systems as a function of δ (with the other potential parameters kept approximately fixed): the electronically labile system is diluted in a large series of solid solvent molecules (frozen solutions

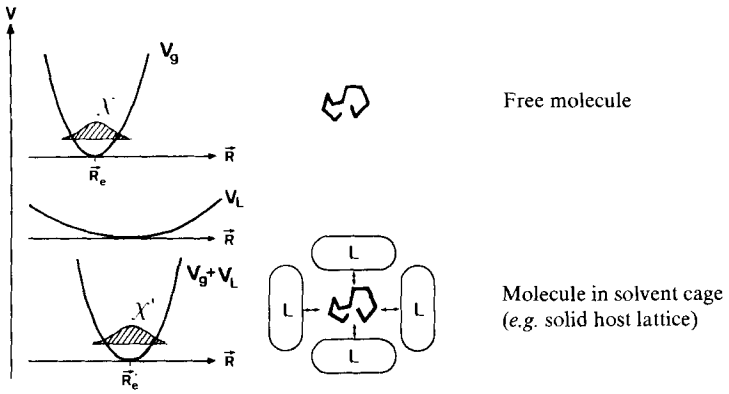

Change of equilibrium structure $\vec{R}_e' \neq \vec{R}_e$

Change of electronic properties because of $\chi'(\vec{R}) \neq \chi(\vec{R})$

$P = \int \langle \psi_{el} | P | \psi_{el} \rangle (\vec{R}) \cdot \chi^2(\vec{R}) \cdot d\vec{R}$

Fig. 4. *Description of the influence of a nonpolar solvent on molecular solute properties in terms of an additive lattice potential $V_L(\vec{R})$*

Table 2. *Vibronic ground state characteristics of various orbitally degenerate metal complexes at 4K in solid solutions*

Examples →	Manganocenes	LS d^5 and d^7-metallocenes		d^1-MX_4	d^9-ML_6	d^5-MX_6
Orbitally degenerate paramagnetic complex	$Mn(cp)_2$ $Mn(R_ncp)_2$	$Mn(cp)_2$ LS $Fe(cp)_2^+$	$Co(cp)_2$ $Ni(cp)_2^+$	VCl_4	CuL_6^{2+} L = H_2O, NH_3	$V(CO)_6$
Diamagnetic host lattices and solvents	$M(cp)_2$, $M(R_ncp)_2$ $M(cp)_2^+X^-$ rare gases, organic solvents	M = Fe, Ru, Mg, Os M = Co, Rh		CCl_4, $TiCl_4$ $GeCl_4$, $SnCl_4$ CBr_4, org. s.	ZnL_6^{2+} MgL_6^{2+} H_2O	$Cr(CO)_6$ $Mo(CO)_6$ $W(CO)_6$
Degeneracy type	spin crossover	*Jahn-Teller* activity				
Coupling case (dim.)	A⊗a (1)	E⊗e (2)				T⊗e, t (2+3)
Symmetry	D_{5h}, D_{5d}			T_d	O_h	
Ground state	$^2E_2 \rightleftarrows {}^6A_1$	$^2E_2(a_1^2e_2^3)$	$^2E_1(a_1^2e_2^4e_2^1)$	$^2E(e^1)$	$^2E(t_2^6e^3)$	$^2T_2(t_2^5)$
Linear *JT* coupling	–	$k^2 \sim 1/2$	$k^2 \sim 1$	$k^2 \sim 3$	$k^2 \sim 10$	$k^2 \leqslant 1$
Second order *JT* significant?	–	no		small	yes	?
First order spin-orbit coupling in open shell?	–	yes		no	no	yes
Behaviour at 4K	localized	delocalized			localized	
Ground state	adiabatic	vibronic			adiabatic	?
ψ-change with δ	discontinuous	continuous (strong)		continuous (weak)	discontinuous	continuous (weak)

or doped single crystals or powders) and the δ-dependence of the electronic ground state observables is determined by spectroscopy (*e.g.* EPR., *Mössbauer*) or magnetic susceptibility. Of course a well defined substitutional site in an isostructural molecular host crystal lattice allows the best quantitative estimate of the solvent potential $V_L(\vec{R})$, *e.g.* from empirical force fields for non-bonded interactions [20]. It is, however, essential to note that important qualitative information on the ground state potential parameters of electronically labile complexes can result already from the general characteristics of the solvent- and temperature-dependence of electronic observables P (continuous or *discontinuous*, see *Fig. 2*), because $V_L(\vec{R})$ will always have a component along the active coordinate(s) R_i of the solute molecule; the contributions of V_L along all the remaining inactive modes (*Fig. 1*, case A) do not influence the electronic properties to a large extent. We have studied pentagonal d^5- and d^7-sandwich complexes, tetrahedral VCl_4 (d^1)-, octahedral copper(II) complexes with CuN_6 and CuO_6 chromophores (d^9) and octahedral $V(CO)_6$ (d^5) in large series of liquid and solid host systems by optical spectroscopy, magnetic susceptibility and EPR. between 4K and room temperature. Characteristic differences in the behaviour of the EPR. spectra under variations of the host lattice and of the temperature could be observed which can be explained in terms of differences in the vibronic coupling type (A $\otimes$ a *vs.* E $\otimes$ e *vs.* T $\otimes$ e, t), of the strength of linear and/or quadratic *Jahn-Teller* coupling and of the effects produced by spin-orbit coupling.

The following examples will be discussed and compared with each other *(Table 2)*:

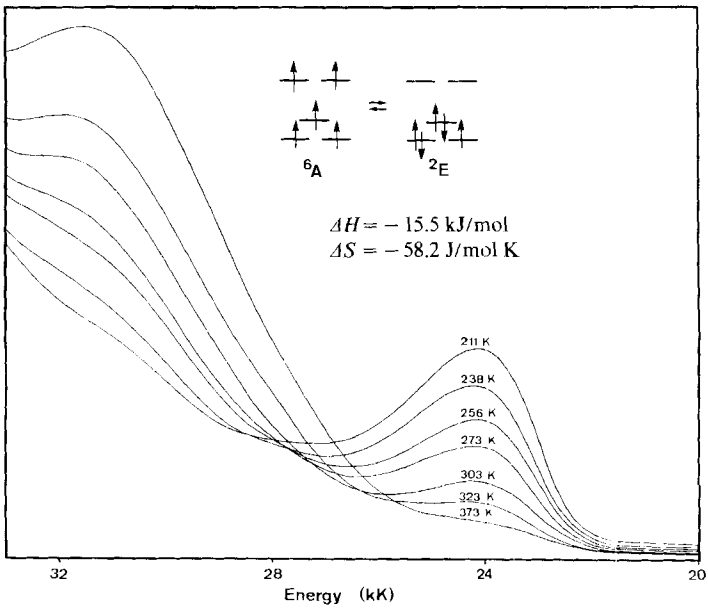

Fig. 5. *Optical absorption spectra of bis-1,1'-t-butyl-cyclopentadienyl-manganese in toluene at various temperatures.* The band at 24 kK corresponds to a $^2E_{2g} \rightarrow {}^2E_{1u}$ charge transfer transition of the low-spin form.

1. $^6A \rightleftarrows {}^2E$ spin crossover of manganocenes [24] [19].
2. E ⊗ e type *Jahn-Teller* molecules with a) fivefold symmetry: d^5- and d^7-metallocenes [19] [25–27], b) tetrahedral symmetry: VCl_4 [21], c) octahedral symmetry: six-coordinate Cu (II) complexes [22].
3. T ⊗ e, t type *Jahn-Teller* molecule: $V(CO)_6$ [23].

2. The high-spin/low-spin equilibrium of the manganocenes. Manganocene and ring-alkylated derivatives show phenomena caused by spin-crossover in gaseous, liquid and solid phases. In the gas-phase evidence resulted from photoelectron spectroscopy [28] and electron diffraction [29]. In liquid solution the equilibria can conveniently be studied by optical spectroscopy *(Fig. 5)* and measurement of the magnetic susceptibility *via* NMR. *(Fig. 6)*. We have extended the earlier studies of *Switzer et al.* [30] by diluting manganocenes with different degrees of ring-alkylation in several organic solvents and by studying the temperature-dependence of the equilibria both by optical and NMR. measurements. The results show that the entropy term is invariably of the order of 50 J/mol K in favour of the high-spin state, and that ΔH favours the low-spin state progressively with increasing ring-

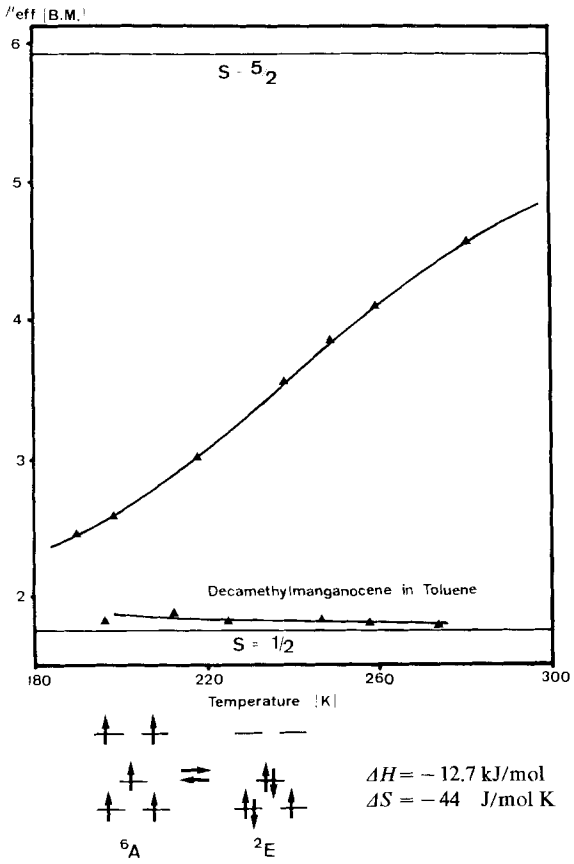

Fig. 6. *T-Dependence of the effective magnetic moment of bis-1,1'-t-butyl-cyclopentadienyl-manganese in toluene determined by the* Evans *NMR. method.* Theoretical spin-only values for the high-spin and low-spin forms are given as horizontal lines. The result for fully methylated $Mn(cp)_2$ is included for comparison.

alkylation [31]. The equilibrium is fast on the NMR. time scale and slow in the optical time scale in liquid solutions, *i.e.* $10^6\ s^{-1} < k < 10^{14}\ s^{-1}$. In solid solutions the solvent influence on the equilibrium is most pronounced, as the solvent potential V_L along the active metal-ring stretching coordinate depends strongly on the packing forces. Dilution in different molecular host lattices favours one or the other spin-state, depending on the space of the solvent cage, as can be seen by EPR. at low temperature [24] [19]. In the case of unsubstituted manganocene diluted in diamagnetic metallocenes the situation is most transparent: magnesocene with the

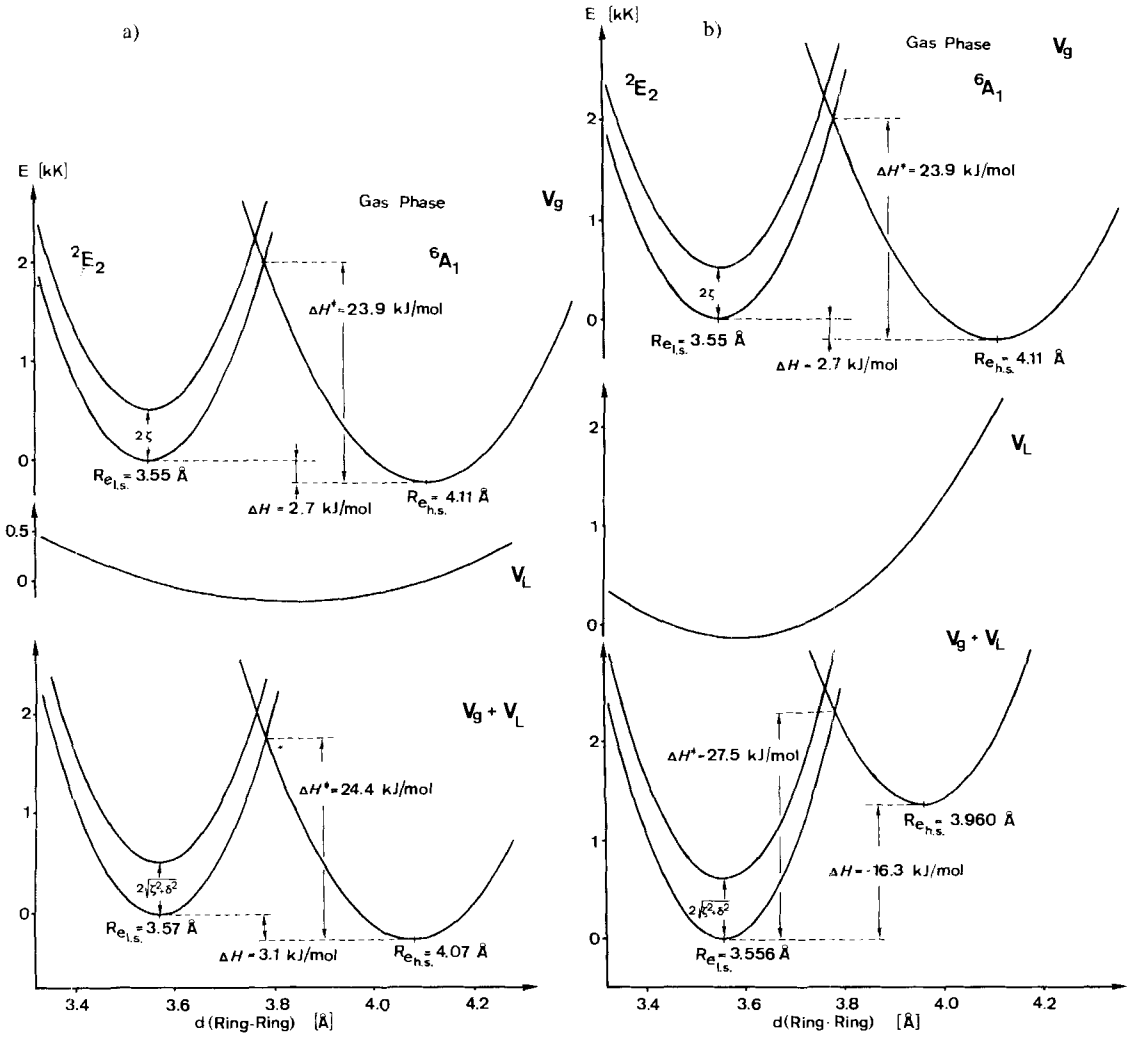

Fig. 7. *Influence of molecular host lattices on the spin equilibrium of $Mn(cp)_2$, described in terms of an additive solvent potential.* V_L has been calculated along ring-ring-stretching coordinate by means of semiempirical force fields. (a) $Mg(cp)_2$ lattice favouring the high-spin form; (b) $Ru(cp)_2$ lattice favouring the low-spin form.

largest metal-to-ring distance favours the high-spin state; ferrocene and ruthenocene having shorter metal-to-ring distances favour the low-spin state. This can be rationalized quantitatively by calculations of V_L from X-ray data of the host [32] [33] by means of empirical force fields [20] assuming an undistorted host lattice [31]. Results are shown in *Figures 7a* and *7b* showing clearly the steric pressure effect of the ruthenocene host relative to the magnesocene lattice-shifting ΔH by almost 20 kJ/mol towards the low-spin side. The approximate gas phase potentials are constructed from *Haalands* electron diffraction data on $Mn(cp)_2$ and

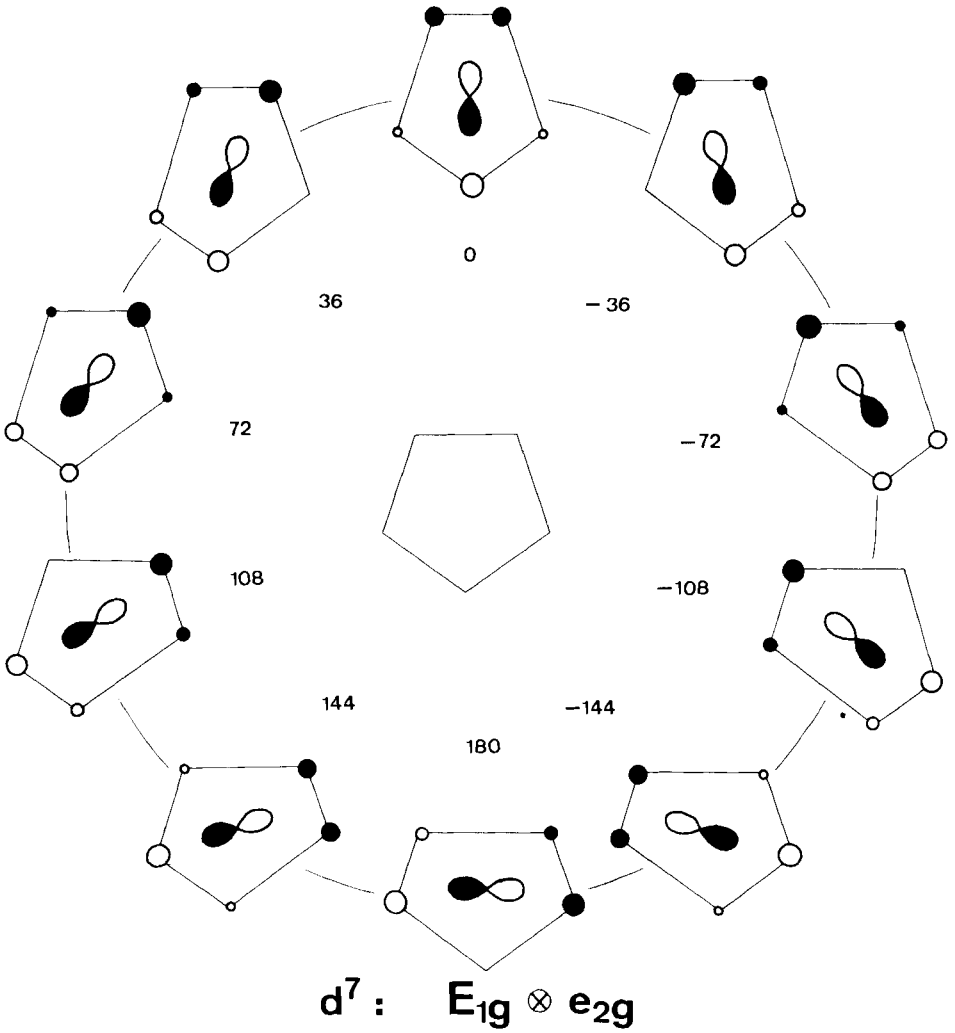

Fig. 8. *Concerted change of molecular and electronic structure of a d^7-metallocene along the* Jahn-Teller *valley of* Figure 1A. A view along the fivefold molecular axis is shown for the case of the e_{2g} C,C-stretching coordinate. Only one ligand ring is shown. Singly occupied LCAO-MO's are indicated schematically.

$Mn(CH_3\text{-}cp)_2$ [29] together with the harmonic force constants from *Raman* data [34]. The high barrier $\Delta H^{\neq}$ of *ca.* 24 kJ/mol explains also the fact that the equilibrium is slow on the EPR. time scale ($k < 10^8$ s^{-1}) at all temperatures; clearly the horizontal displacement ΔR is much larger than the zero-point amplitude, *i.e.* the spin-crossover of the manganocenes belongs to the localized case 1 in *Figure 2.*

3. E ⊗ e Type *Jahn-Teller* molecules. – *a) Fivefold symmetry: d^5- and d^7-metallocenes.* Both low spin d^5-metallocenes (as manganocene and ferricenium cation) and d^7-metallocenes (as cobaltocene and nickelicenium cation) are *Jahn-Teller*-active and belong to the E ⊗ e coupling class with first order spin-orbit coupling *(Table 2).* EPR. results in various host lattices obtained at low temperatures have been reported earlier [19] [25–27]. In the d^5-case the e_{1g} ring-tilt mode shows the largest coupling, in the d^7-case there are three modes of comparable activity, the out-of-plane e_{2g} mode dominating *(Fig. 9). Figure 8* illustrates the fact

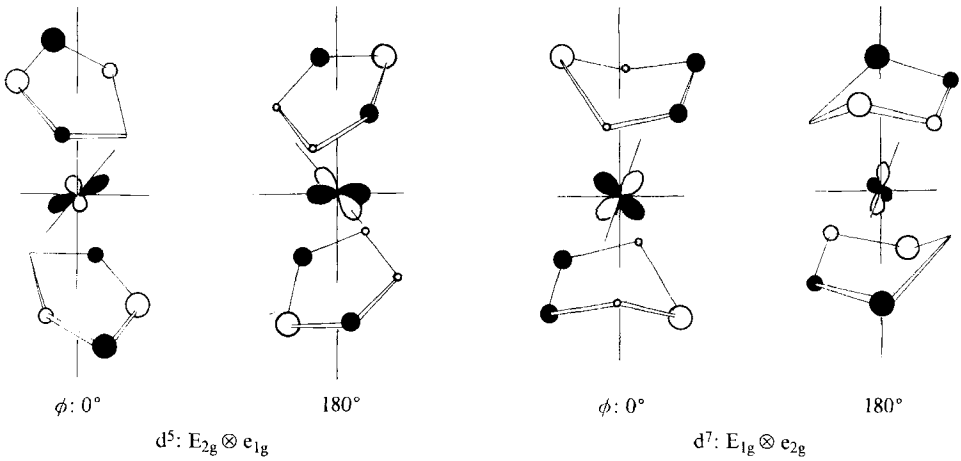

Fig. 9. *Side view of* Jahn-Teller *active vibrations of d^5- and d^7-metallocenes.* Amplitudes of singly occupied orbitals on the ring C-atoms are symbolized by black and white circles with variable size. Left: e_{1g} ring-tilt mode, active for d^5; right: e_{2g} out-of-plane distortion, active for d^7.

that there is a continuum of energetically equivalent conformations along the circular *Jahn-Teller* valley of *Figure 3,* and that the coupling of the electronic and nuclear motion can be rationalized in terms of relatively simple LCAO/MO arguments: for d^7-metallocenes with a singly occupied e^*_{1g} antibonding orbital the e_{2g} C,C-stretching distortion maximizes the C,C-bond order while the e_{2g} out-of-plane ring distortion minimizes the negative contributions to the metal-to-carbon bond order (see also [27] and *Fig. 4*). As shown in *Figure 10* for the example of cobaltocene the magnetic parameters change quite drastically along the matrix series; there is a continuous dependence on the asymmetry parameter δ introduced by the lattice potential V_L along the *Jahn-Teller* modes as shown in *Figure 11* for the case of the out-of-plane distortion mode S_{13} in a one-dimensional cross section. The corresponding two-dimensional view is shown in *Figure 12,* together with the

vibrational density distribution χ^2 for the ground *Kramers* doublet exhibiting axial symmetry in the free molecule, but becoming more and more asymmetric and localized with increasing δ. A qualitative view of the stepwise distortion of the shape of the *Mexican-hat* potential along a matrix series producing increasing values of δ is given in the four 1-dimensional model cross sections of *Figure 13*. A somewhat less formal description of the effect of the steric hindrance of the molecular environment on the *Jahn-Teller* motion of a solute molecule in a solid solution is shown in *Figure 14* for the case of the ring-tilt mode in d^5-metallocenes [23].

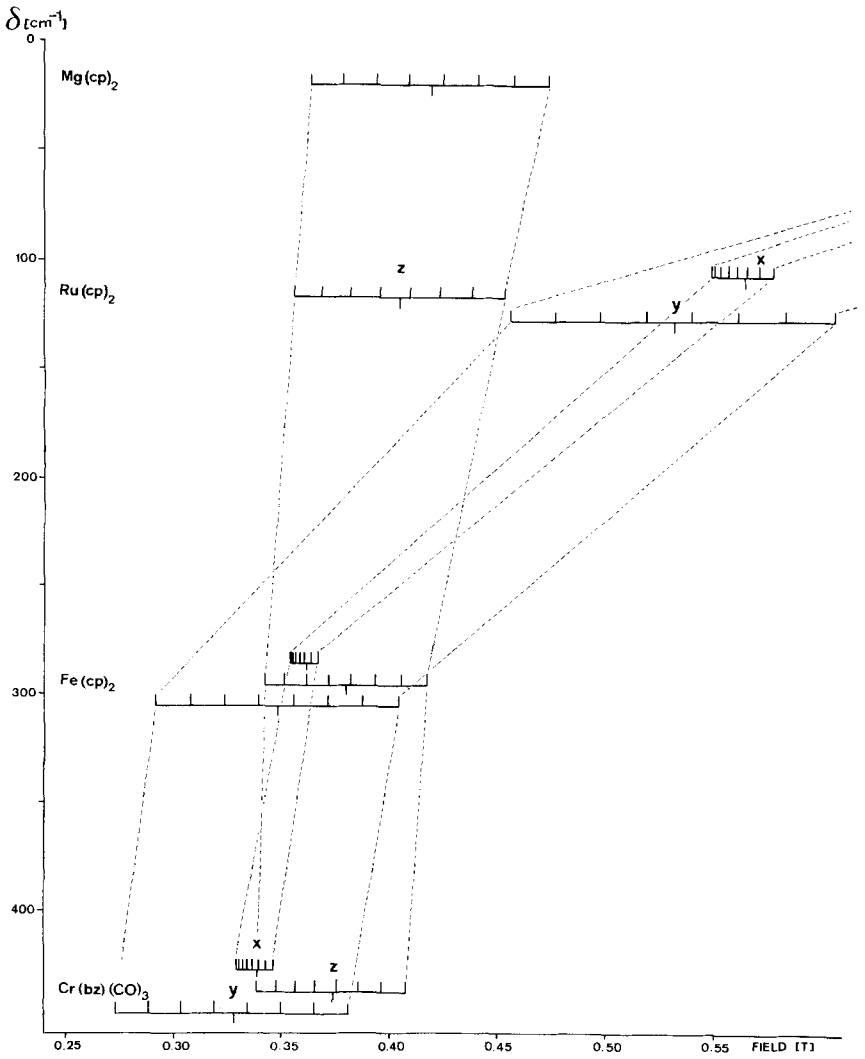

Fig. 10. *Experimental host lattice dependence of the g and metal hyperfine tensors of cobaltocene.* Stick diagrams of principal axes EPR. spectra for four selected host systems with widely differing asymmetries δ. EPR. data are taken from [19]. x and y spectra for $Co(cp)_2$:$Mg(cp)_2$ are off-scale on the high field side.

This strong continuous dependence of magnetic properties on the lattice parameter δ contrasts with the discontinuous behaviour of the spin-crossover example discussed earlier as well as with the subsequent E ⊗ e type *Jahn-Teller* molecules to be discussed below. The reason is the first-order spin-orbit coupling between the two equivalent electronic functions lifting the electronic degeneracy already in the free molecule. The continuous dependence of all electronic properties on δ can be understood as follows: The ground vibronic *Kramers* doublet of these d^5- and d^7-sandwich molecules has to be described by a complex vibronic superposition of the general form

$$\psi = c_I \phi_I \chi_I + i c_{II} \phi_{II} \chi_{II} \tag{1}$$

where the c_I and c_{II} are coefficients ($c_I^2 + c_{II}^2 = 1$), the ϕ_i are orthogonal electronic wavefunctions and the χ_i are the overlapping vibrational wavefunctions with $\langle \chi_I | \chi_{II} \rangle = V$. In the free molecule ($\delta = 0$) $c_I^2 = c_{II}^2 = 1/2$; both the vibrational density χ^2 and the electronic charge density ϕ^2 show axial symmetry. In asymmetric

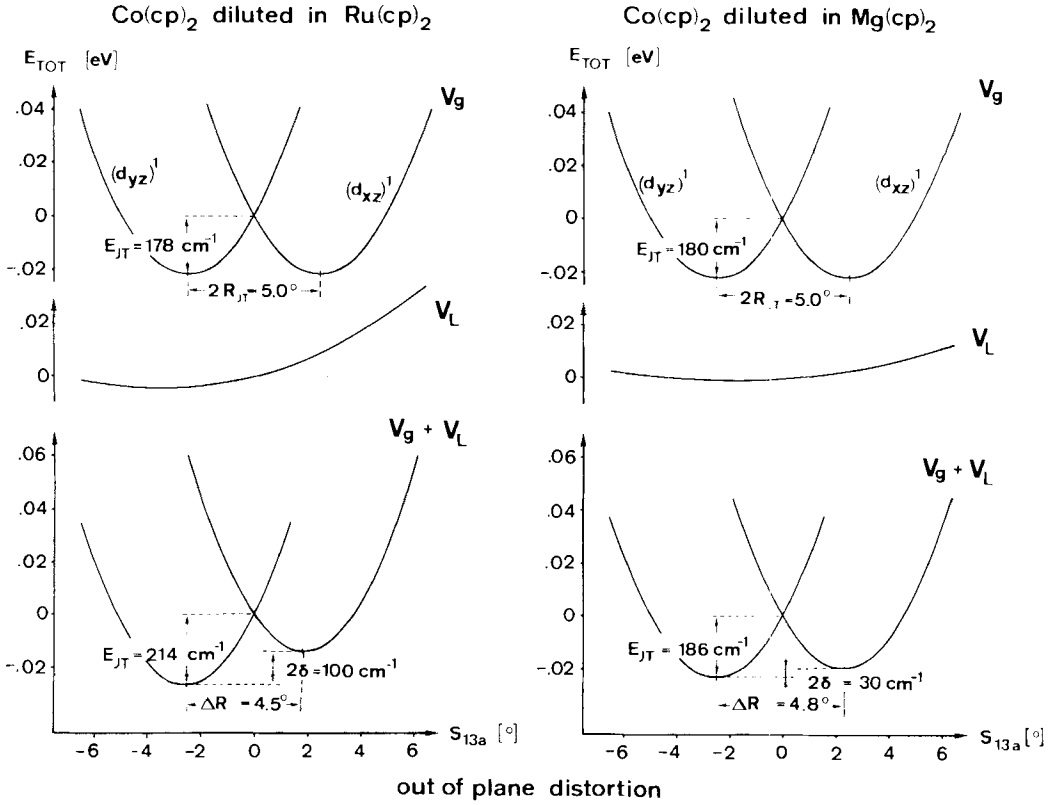

Fig. 11. *Influence of Ru(cp)$_2$ and Mg(cp)$_2$ host lattices on the* Jahn-Teller *diameter* ΔR *and on the asymmetry parameter* δ *of Co(cp)$_2$ described in terms of an additive solvent potential* V_L. V_L has been calculated along the out-of-plane e_{2g}-distortion coordinate S_{13} of *Figure 9* by means of semiempirical force fields.

potentials c_I^2 and c_{II}^2 become increasingly different, depending on the ratio δ/ζ whereby ζ is an appropriate spin-orbit coupling parameter.

Defining an asymmetry parameter a by the equation

$$\tan a = \frac{c_I^2 - c_{II}^2}{2\, c_I c_{II}} \approx -\frac{2\delta}{n\zeta}; \qquad n = \begin{cases} +2 \text{ for } d^5 \\ -1 \text{ for } d^7 \end{cases} \tag{2}$$

one obtains the following first-order expression for the g values [19]:

$$g_\parallel = g_z = 2(1 + n\, k_\parallel V \cos a) \tag{3}$$

$$g_\perp = \tfrac{1}{2}(g_x + g_y) = 2 \sin a \tag{4}$$

$k_\parallel$ is an orbital angular momentum reduction factor resulting from covalency being of the order of 0.8 in the case of cobaltocene, nickelicenium and low-spin

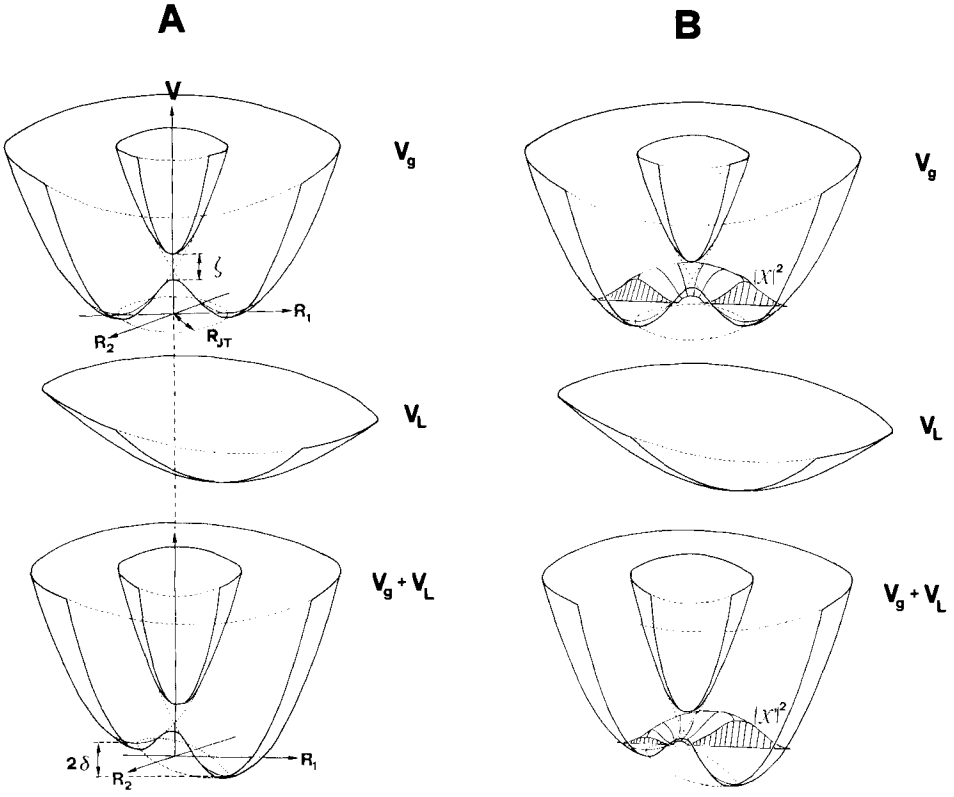

Fig. 12. *Influence of an asymmetric solvent field V_L on potential surface and nuclear density distribution $|\chi|^2$ of the lowest vibronic state of an $E \otimes e$-type* Jahn-Teller *molecule with first-order spin-orbit coupling for* $E_{JT} \approx \hbar\omega \approx \zeta \approx 2\delta$ ($R_{JT} = \frac{1}{2}\,\Delta R =$ *Jahn-Teller* radius, $\zeta =$ spin-orbit splitting, $2\delta =$ energetic asymmetry introduced by a lattice potential V_L).

(A) shows the potentials without and (B) together with the vibrational density distribution $\chi^2(\vec{R})$ of the vibronic ground state.

manganocene. V is a vibronic reduction factor *(Ham factor)* decreasing with increasing dynamic *Jahn-Teller* motion [35], and ζ is the effective spin-orbit coupling parameter, being of the order of 300 cm^{-1} in the three cases considered above. While δ was found to vary between as little as 40 cm^{-1} and several thousands of wavenumbers [19] and therefore to be responsible for most of the host lattice dependence of the g values, the *Ham factor* V also showed a significant increase from 0.3 (for $\delta = 0$) towards unity for large δ. This gradual suppression of dynamic *Jahn-Teller* motion by asymmetric host lattice potentials is illustrated schematically

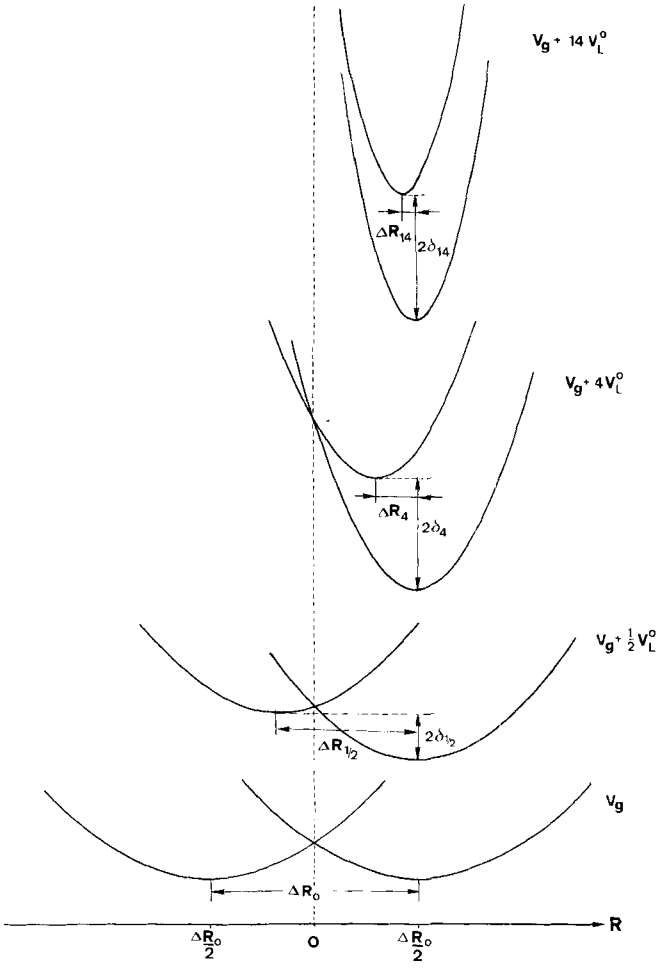

Fig. 13. *Explanation of the observed decrease of dynamic* Jahn-Teller *coupling of d^5- and d^7-sandwich complexes with increasing asymmetry δ in terms of both an increased effective force constant and a reduced horizontal displacement ΔR by asymmetric lattice potentials V_L with increasing curvature from bottom (free molecule) to top (static limit).* For simplicity in this one-dimensional cross section V_L has been chosen harmonic and displaced from origin by one *JT*-radius, *i.e.* $V_L = \frac{1}{2} f_L\,(R - \Delta R/2)^2$ with $f_L = 0.1/2.4$ and 14 times the force constant of the free molecule.

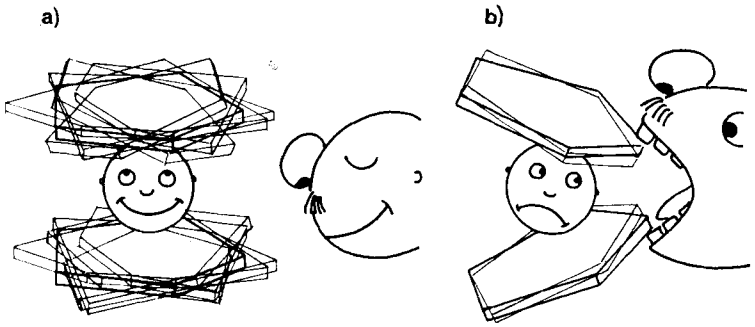

Fig. 14. *Illustration of the matrix effect explained* in Figures 11–13: *suppression of the dynamic* Jahn-Teller *ring tilt motion* (Fig. 9) *of free gaseous* d^5*-metallocenes* (a) *by an asymmetric molecular environment in a host lattice* (b).

in the one-dimensional cross sections of *Figure 13*. While for linear host lattice potentials V_L a decrease of V with δ is predicted by theory [36], nonlinear potentials tend to decrease the horizontal spacing ΔR with increasing δ and thereby increase the vibrational overlap V towards unity. This effect of ΔR-reduction is indeed predicated from our V_L calculations as in the example shown in *Figure 11*.

b) Tetrahedral symmetry: Vanadium Tetrachloride (d^1). Similar to d^5- and d^7-metallocenes VCl_4 is an $E \otimes e$ type *Jahn-Teller* molecule with moderate linear coupling, *i.e.* with a *Jahn-Teller* energy comparable to a vibrational quantum $E_{JT} \approx \hbar\omega \approx 100$ cm^{-1} [37]. The single degenerate active mode is depicted in *Figure 15*. Dilution in a variety of tetrahedral and other host systems and subsequent EPR. analysis at low temperatures produced results quite different from the sandwich case. Little matrix-dependence was observed; all matrices gave spectra similar to the one shown in *Figure 16*, interpretable in term of almost axially symmetric g and A tensors [21]. Similar spectra had been obtained earlier [38] [39].

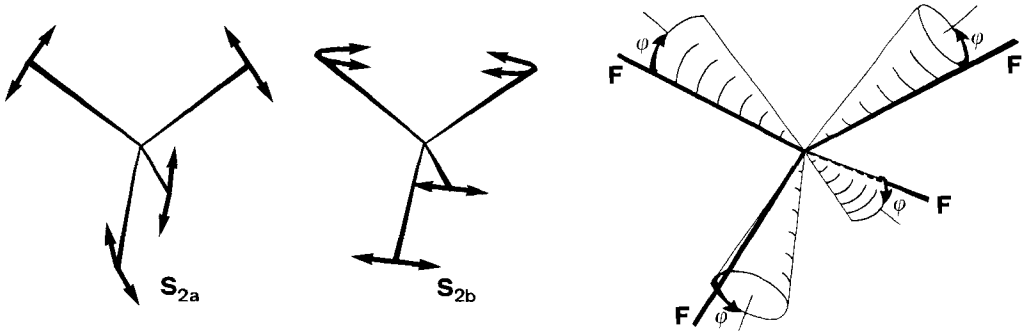

Fig. 15. *Dynamic* Jahn-Teller *effect in* VCl_4. Left: perspective view of the two degenerate components of the active e bending mode; right: nuclear motion along the *Jahn-Teller* valley of *Figure 3A*. ($\phi = 0°$ (strong solid lines): flattened tetrahedron (F), $\phi = 180°$: elongated tetrahedron, $\phi = 90°$ and 270° twisted tetrahedron).

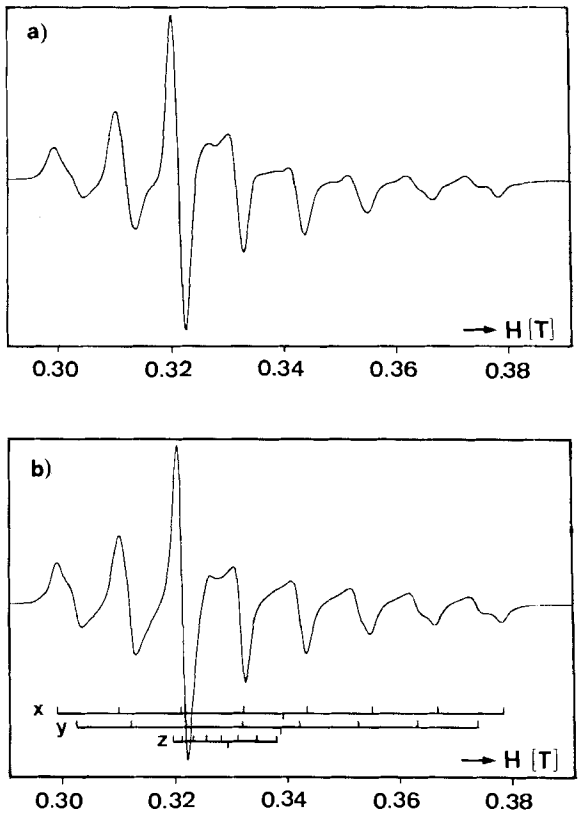

Fig. 16. *EPR.-spectrum of VCl_4 in frozen cyclohexane* ($\nu = 9.08476$ GHz; a) experimental spectrum at 4K b) calculated spectrum (linewidth = 1.2 mT)).

The g values are consistent with a vibronic ground state of the form

$$\psi = \sin\alpha \mid 3\,d_{z^2} > \chi_I + \cos\alpha \mid 3\,d_{xy} > \chi_{II} \tag{5}$$

with $\langle \chi_I | \chi_{II} \rangle = 0$ and α invariably close to 60°, almost independent of the matrix (see *Table 3*).

This means that the weight ratio of the two electronic functions is always close to 3:1 in favour of d_{z^2} corresponding to a stabilization of the flattened relative to the elongated tetrahedron. This result contrasts with the pronounced δ-dependence of the mixing angle α in the case of the metallocenes. It is in fact predicted by theory

Table 3. *Vibronic mixing angle α from EPR. data of VCl_4 in several host systems at 4K*

Host lattice	α [degrees]	Host lattice	α [degrees]
CCl_4	57.6 (0.5)	Toluene	58.4 (2.0)
Cyclohexane	58.7 (3.0)	$GeCl_4$	60.5 (0.8)
CBr_4	54.7 (3.0)	$TiCl_4$	57.6 (1.5)
$SnCl_4$	57.3 (1.6)	Average	57.7

[35] and is explained by the absence of spin-orbit coupling between the two degenerate electronic functions [21] (see *Fig. 17*). For the potential and the density distribution of the lowest *Kramers* doublet *(Fig. 12)* applies equally well to VCl_4 as to the metallocenes; the only difference consists in the fact that the real crossing (broken lines) takes place instead of the avoided crossing (solid lines).

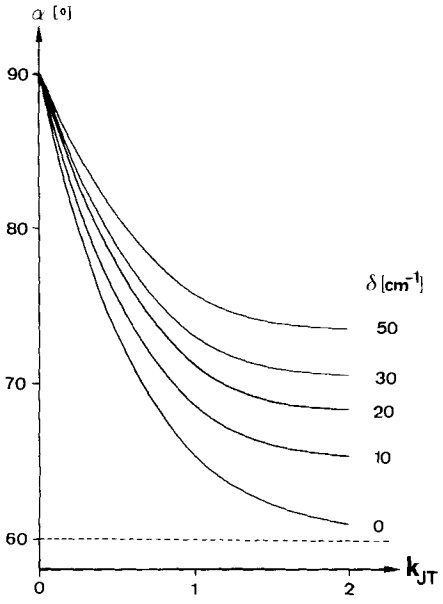

Fig. 17. *Theoretical vibronic mixing angle α for various linear* Jahn-Teller *coupling parameters k_{JT} and host lattice asymmetry fields δ, calculated within a harmonic first order model as described in [25] with $\hbar\omega = 100\ cm^{-1}$ and $\zeta = 0$.* Inclusion of moderate second order ('warping') terms does not modify the picture to a large extent [21]. Since a limited set of 30 harmonic oscillator functions has been used convergence is obtained only for $0 < k_{JT} < 1$. In the limit of strong linear JT coupling ($k_{JT} \gg 1$) an asymptotic value of $\alpha = 60°$ is predicted [35], irrespective of δ. In the case of negative δ (favouring an elongated tetrahedron) α has to be replaced by $(90° - \alpha)$.

c) Octahedral symmetry: six-coordinate Cu(II) complexes (d^9). The *Jahn-Teller* effect in six-coordinate copper(II) complexes is very well documented in the literature [2–6] [22] [40] and needs no detailed discussion here. In spite of the formal similarity to the VCl_4 case the nature of the ground state of CuL_6 complexes in low-symmetry environments is completely different, because both linear and quadratic coupling energies are larger than the zero-point energy. Very small δ values are sufficient to freeze CuL_6 complexes in a static distortion; even in case of cubic sites in molecular crystals static distortion occurs because of the random strain caused by imperfections [2]. For a quite large range of δ values the ground *Kramers* doublet can be written as a single *Born-Oppenheimer* product of a $d_{x^2-y^2}$-hole multiplied by a well-localized harmonic oscillator vibrational function. Substantial lattice potentials (with minima not coinciding with the tetragonal-elongation conformations of the free CuL_6 cluster) are required for significant (nonvibronic!) d_{z^2}-admixtures to the ground state hole [22].

Of course the contrasts mentioned between the solvent-dependence of the three types (2 a-c) of $E \otimes e$ *Jahn-Teller* molecules holds only for low temperatures at which exclusively the ground *Kramers* doublet is populated. In the high-temperature limit the behaviour is very similar: for $kT \gtrsim E_{JT}$ rapid dynamic *Jahn-Teller* motion

within the whole space of the *Mexican-hat* potential takes place and all the subtle differences introduced by spin-orbit coupling and warping terms are wiped out.

4. $V(CO)_6$, a $T \otimes e$, t Coupling type molecule. – Octahedral vanadium hexacarbonyl has a $(t_{2g})^5$-configuration and therefore a triply degenerate electronic ground state, split by spin-orbit coupling. If only coupling to the e-stretching mode is considered the surface of *Figure 3B* applies and a strong disposition to permanent tetragonal distortion is expected.

However trigonal distortions are also *Jahn-Teller*-active and a five-dimensional surface has to be considered [41] [42]. We have diluted $V(CO)_6$ in the isostructural diamagnetic hosts of $Cr(CO)_6$, $Mo(CO)_6$ and $W(CO)_6$ and have studied the EPR. spectra at low temperature both in single crystals and powders [21] [23]. We found orthorhombic magnetic tensors in all three lattices; the tensor axes do not correspond neither to purely tetragonal nor to purely trigonal distortions indicating a complicated situation with comparable e and t_2 coupling-strength as found earlier in the case of $Mn(CN)_6^{4-}$ [43]. Also we found drastic changes of the spectra with temperature which we have not understood yet. From the evidence accummulated so far for $(t_{2g})^5$-molecules the experimental information is not sufficient for an unambiguous description. It is not even completely clear whether the ground level has to be described by a BO-product or a vibronic superposition. The moderate matrix-dependence seems to favour the adiabatic alternative.

Table 4. *EPR. parameters of $V(CO)_6$ at 4K*[a])

Host lattice	g_x	g_y	g_z	A_x	A_y	A_z
$Cr(CO)_6$	2.134	2.110	1.983	43.3	49.9	26.1
$Mo(CO)_6$	2.127	2.112	1.978	42.6	51.4	24.1
$W(CO)_6$	2.126	2.120	1.980	43.3	50.6	24.9

[a]) ^{51}V hyperfine values in units of 10^{-4} cm^{-1}; linewidth ~ 10 Gauss.

5. Concluding Remarks. – From the above examples it is apparent that a systematic study of the host lattice dependence of EPR. spectra of electronically labile molecules can be of substantial help for the characterization of the nature of the vibronic ground state and its relation to the shape of the lowest potential surface. While some progress has been made in the case of *Jahn-Teller* and spin-crossover molecules, systematic studies of the solvent dependence of the electronic properties of mixed valence compounds and exchange coupled systems have hardly begun. We hope that the situation will change in the near future.

This work has been supported by the *Swiss National Science Foundation* (Project Nr. 2.683.0.80).

Experimental Part

Preparation of samples. All the investigated air- and moisture-sensitive paramagnetic sandwich compounds, VCl_4 and $V(CO)_6$ were either purchased *(Research Inorganic Chemicals)* or prepared following methods from the literature. Details of the preparative work are described elsewhere [19] [21a] [23] [25]. Single crystals and powders of diluted paramagnetic complexes (*ca.* ½% for EPR. and magnetic susceptibility studies) were obtained by vacuum cosublimation [25] or by coprecipitation from solution [21a] [23].

EPR. measurements. X-Band EPR. spectra were measured on a *Varian* E-Linie spectrometer fitted with an *Oxford* liquid helium cryostat and variable temperature accessory. The magnetic field was calibrated using an NMR. gaussmeter and the microwave frequency was measured using a frequency counter. In single crystal studies g and metal hyperfine tensors were obtained by *Schonlands* procedure [44]. In the case of frozen solutions and diluted powders the spectra were simulated by a computer program [45].

Optical spectra and magnetic susceptibility studies. Optical spectra of liquid solutions and glasses were recorded on a *Beckmann* Acta M7 spectrometer (range 250 nm-3000 nm). Magnetic susceptibilities in solution were determined by a modification of the *Evans* [46] NMR. method on a *Bruker* HX 90 spectrometer. *Coaxial* NMR.-cells from *Wilmach Glass Company* were used.

REFERENCES

[1] *J.H. Ammeter*, Nouv. J. Chim. *4*, 565 and 631 (1980).
[2] *M.D. Sturge*, Solid State Phys. *20*, 91 (1968).
[3] a) *R. Englman*, 'The Jahn-Teller Effect in Molecules and Crystals', Wiley, New York, 1972; b) *C.J. Ballhausen*, 'Molecular Electronic Structures of Transition Metal Complexes', McGraw-Hill 1979.
[4] *D. Reinen & C. Friebel*, Structure and Bonding *37*, 1 (1979).
[5] *I.B. Bersuker*, Coord. Chem. Rev. *14*, 357 (1975).
[6] *M.C.M. O'Brien*, Proc.Roy. Soc. *A 281*, 323 (1964).
[7] *P. Gütlich*, J. Physique *40*, Colloque C2, C2-378 (1979).
[8] *E. König*, Ber. Bunsenges. Physik. Chem. *76*, 975 (1976).
[9] *R. Morassi, I. Bertini & L. Sacconi*, Coord. Chem. Rev. *11*, 343 (1973).
[10] a) *M.B. Robin & P. Day*, Adv. Inorg. Chem. Radiochem. *10*, 247 (1967); b) *P. Day*, 'Mixed Valence Compounds', D.B. Brown ed., D. Reidel, 1980, p. 3; c) *A. Ludi*, ibid, p. 25.
[11] *S.B. Piepho, E.R. Krausz & P.N. Schatz*, J. Am. Chem. Soc. *100*, 2996 (1978).
S.B. Piepho, Nouv. J. Chim. *4*, 639 (1980).
[12] *T.J. Meyer*, Acc. Chem. Res. *11*, 94 (1978) and Chem. Phys. Letters *64*, 417 (1979).
[13] *G.C. Allen & N.S. Hush*, Progr. Inorg. Chem. *8*, 357 (1967).
[14] a) *W.E. Hatfield*, Inorg. Chem. *15*, 2107 (1976); b) *A. Bencini & D. Gatteschi*, Inorg. Chim. Acta *31*, 11 (1978).
[15] *H.U. Güdel, U. Hauser & A. Furrer*, Inorg. Chem. *18*, 2730 (1979).
[16] a) *P.J. Hay, J.C. Thibeault & R. Hoffmann*, J. Am. Chem. Soc. *97*, 4884 (1975); b) *G. van Kalkeren, W.W. Schmidt & R. Block*, Physica *B 97*, 315 (1979).
[17] a) *O. Kahn & B. Briat*, J. Chem. Soc. Faraday Trans. II 7, 268 (1976); b) *O. Kahn & M.F. Charlot*, Nouv. J. Chim. *4*, 567 (1980).
[18] a) *C. Daul, C.W. Schläpfer & A.v. Zelewsky*, Structure and Bonding *36*, 129 (1979); b) *L. Banci, A. Bencini, C. Benelli & D. Gatteschi*, Nouv. J. Chim. *4*, 593 (1980).
[19] *J.H. Ammeter*, J. Magn. Reson. *30*, 299 (1978).
[20] See *e.g.*: *S.R. Niketic & K. Rasmussen*, 'The Consistent Force Field: A Documentation' 'Lecture Notes in Chemistry', Vol. 3, Springer-Verlag, Berlin 1977.
[21] a) *E.R. Deiss*, Dissertation ETH, Zürich 1980; b) *R. Meyer, M. Bacci, E.R. Deiss & J.H. Ammeter*, unpublished 1981.
[22] a) *J.H. Ammeter, H.-B. Bürgi, E. Gamp, V. Meyer-Sandrin & W.P. Jensen*, Inorg. Chem. *18*, 733 (1979); b) *E. Gamp*, Dissertation ETH, Zürich 1980.

[23] *R. Bucher*, Dissertation ETH, Zürich 1977.
[24] *J. H. Ammeter, R. Bucher & N. Oswald*, J. Am. Chem. Soc. *96*, 7833 (1974).
[25] *J. H. Ammeter & J. D. Swalen*, J. Chem. Phys. *57*, 678 (1972).
[26] *J. H. Ammeter & J. M. Brom*, Chem. Phys. Lett. *27*, 380 (1974).
[27] *J. H. Ammeter, N. Oswald & R. Bucher*, Helv. Chim. Acta *58*, 671 (1975).
[28] *S. Evans, M. L. H. Green, B. Jewitt, G. H. King & A. F. Orchard*, J. Chem. Soc. Faraday Trans. II *70*, 356 (1974).
[29] *A. Almenningen, S. Samdal & A. Haaland*, J. Chem. Soc. Chem. Commun. *1977*, 14.
[30] *M. E. Switzer, R. Wang, M. F. Rettig & A. H. Maki*, J. Am. Chem. Soc. *96*, 7669 (1974).
[31] *J. H. Ammeter, J. Bachmann & Ph. Baltzer*, unpublished (1980).
[32] *W. Bünder & E. Weiss*, J. Organomet. Chem. *92*, 1 (1975).
[33] *J. D. Dunitz & P. Seiler*, Acta Crystallogr. *B 35*, 1068 (1979).
[34] *V. T. Aleksanyan & B. V. Lokshin*, J. Organomet. Chem. *131*, 113 (1977).
[35] a) *F. S. Ham*, Phys. Rev. *A 138*, 1727 (1965); b) *F. S. Ham*, ibid. *166*, 307 (1968).
[36] a) *N. Oswald*, Dissertation ETH 1977; b) *N. Oswald & J. H. Ammeter*, unpublished (1977).
[37] a) *Y. Morino & H. Uehara*, J. Chem. Phys. *45*, 4543 (1966); b) *C. J. Ballhausen & A. D. Liehr*, Acta Chem. Scand. *15*, 775 (1961); c) *C. J. Ballhausen & J. deHeer*, J. Chem. Phys. *43*, 4304 (1965).
[38] *D. W. Pratt*, Lawrence Radiation Laboratory Report UCRL-17406 University of California, Berkeley, California 1967.
[39] *R. B. Johannesen, G. A. Candela & Tung Tsang*, J. Chem. Phys. *48*, 5544 (1968).
[40] a) *I. Bertini, D. Gatteschi & A. Scozzafara*, Coord. Chem. Rev. *29*, 67 (1979); b) *V. E. Petrashen, Yu. V. Yablokov & R. L. Davidovich*, Phys. Stat. Sol. (b) *101*, 117 (1980) and references therein; c) *J. S. Wood, C. P. Keijzers, E. deBoer & A. Buttafava*, Inorg. Chem. *19*, 2213 (1980).
[41] a) *M. C. M. O'Brien*, Phys. Rev. *187*, 407 (1969); b) *A. Ranfagni, D. Mugnai, M. Bacci, M. Montagna, O. Pilla & G. Viliani*, Phys. Rev. *B20*, 5358 (1979) and references therein.
[42] *M. Bacci*, Chem. Phys. *40*, 237 (1979).
[43] *B. Bleaney & M. C. M. O'Brien*, Proc. Phys. Soc. *B63*, 1216 (1956).
[44] *D. S. Schonland*, Proc. Phys. Soc. *73*, 788 (1959).
[45] *C. Daul, C. W. Schläpfer, B. Mohos, J. H. Ammeter & E. Gamp*, Comp. Phys. Comm. *21*, 385 (1981).
[46] *D. F. Evans*, J. Chem. Soc. *1959*, 2003.